International Journal of Engineering &Technology, 7 (4) (2018) 6458-6463

International Journal of Engineering & Technology

Website: www.sciencepubco.com/index.php/IJET
doi: 10.14419/ijet.v7i4.23298
Research paper

Design of low-cost and high-speed portable two-dimensional electrical impedance tomography (EIT)

Widodo Aris, Endarko *

Department of Physics, Institut Teknologi Sepuluh November, Kampus ITS Sukolilo - Surabaya, 60111, East Jawa, Indonesia
**Corresponding author E-mail: endarko@physics.its.ac.id*

Abstract

Electrical Impedance Tomography (EIT) is a non-invasive of biomedical imaging technique that used constant electric current as a signal modality. The main proposed study was to design two-dimensional EIT system that could support high speed for detection of anomalies inside the practical phantom and has a low cost in fabrication. High-speed portable two-dimensional EIT has been successfully designed and fabricated to generate a reconstructed image from data acquisition in the practical phantom with 16 electrodes. The manufactured EIT equipped with a 7-inch screen as monitoring display, Raspberry Pi 3 Model B and Arduino Uno as controlling and processing units. The system was also used Gauss-newton method for image reconstruction that using Phyton programming which embedded into Raspberry Pi 3 Model B. The results showed that the portable EIT system produced a high-speed data acquisition and image reconstruction with a process is less than 7 seconds. The manufactured EIT revealed that the system had a potential application for medical imaging.

Keywords: *Raspberry Pi; Arduino Uno; Electrical Impedance Tomography (EIT); High-Speed; Low-Cost.*

1. Introduction

Electrical Impedance Tomography (EIT) is a new medical imaging technique that used electrical signals as the primary modality and has been used in various fields such as industry, geophysics, and medical [1]. In the medical field, EIT can be applied due to has the advantage of being cheap, portable and not harmful to the tissues of the human body [2], and can be used to display the anatomical image of the human body, observe the functional organs of the body and some applications of life support equipment [3].

EIT could not damage human body tissues due to use low energy compared to CT scan that using radioactive materials in its operations [4]. EIT operated with the constant electric current at 1 mA 20 kHz which injected into the body or phantom through electrodes. This electric current is so weak that it will not give a shocking sensation or burn body tissues as in the symptoms of electric shock [5]. The measured voltage resulted from injecting an electric current will be converted to a digital signal using Analog to Digital converter (ADC) to be processed on the control unit which then used for image reconstruction [6].

The main design of the EIT system involved hardware and software development. Fabrication of hardware focuses on high-frequency constant current source 1 mA that capable of supporting high impedance due to human body tissue has a high impedance [7], and produce a good image reconstruction.

Moreover, the software design involved algorithms in processing the measured voltage data into a reconstruction image [8]. Algorithm design required a physics and mathematical approach based on predetermined boundary conditions for objects to be reconstructed. Physics approach is focused on physical phenomena that occur when electric currents pass through body tissues or phantoms by applying physical laws in it, such as Maxwell's law and Kirchhoff's law [9]. The mathematical approach focused on the phantom model approach and the search for a mapping solution for the conductivity distribution resulting from the processing of the boundary voltage data measured by hardware [3]. The finite element method (FEM) used to conductivity mapping based on the mesh generated from the phantom model. Various algorithms that are often used in EIT, namely Gauss-Newton algorithm and back projection algorithm [10]. In each algorithm gives its characteristics on the results of image reconstruction. Gauss-newton will produce Gaussian distribution, whereas the back projection provides a shadow projection image [11]. All algorithms are arranged in a programming language so that they can interact with hardware [12]. In the present study, we proposed the low-cost portable EIT with high-speed acquisition data and image reconstruction using Raspberry Pi 3 Model B and Arduino Uno for processing and controlling units and a 7-inch screen for displaying reconstructed image. The fast imaging with the highly precise image reconstruction will also be evaluated using Gauss-newton method with the practical phantom in the circle form with 16 electrodes.

2. Fabrication of portable electrical impedance tomography

2.1. Hardware design

Figure 1 shows a block diagram of EIT. The main component for designing the functionality of EIT divided into several blocks of circuits namely voltage controlled current source (VCCS) as a supply a constant current source at 1 mA with a frequency of 20 kHz. A multiplexer as a high-speed digital switch for injecting current and capture the voltage boundary response, voltage measurement along with Analog to Digital Converter (ADC) and control unit as a circuit controller and voltage data processor.

Copyright © 2018 Widodo Aris Endarko. This is an open access article distributed under the Creative Commons Attribution License, which permits unrestricted use, distribution, and reproduction in any medium, provided the original work is properly cited.

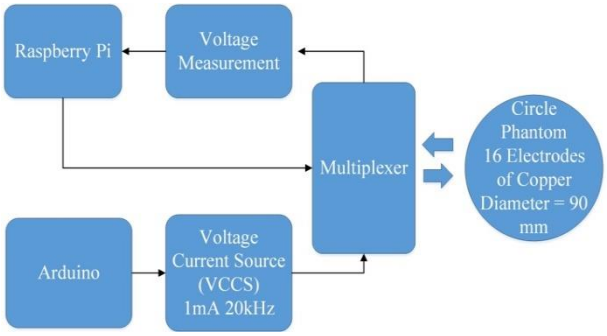


Fig. 1: Design of Electrical Impedance Tomography with the High-Speed System.

The EIT system has two control units, namely Arduino and Raspberry Pi, as shown in Figure 1. Arduino has a role as a control system for voltage current source (VCCS) in ensuring a constant supply of electric current for injection in the practical phantom. Meanwhile, a Raspberry act as a control unit and data processor in the EIT system for data acquisition and image reconstruction. The explanation of the system per block will be discussed in the following section.

2.1.1. VCCS design

The VCCS design in the EIT system is shown in Figure 2. The part of the VCCS consists of a voltage controlled oscillator (VCO) as a signal generator circuit using IC AD9850 Direct Digital Synthesizer (DDS), non-inverting amplifier, the fourth order Butterworth Bandpass Filter with a Sallen-Key topology and Triple Op-Amp (TOA) current source circuit for voltage to current converter (VCC) using IC AD844AN.

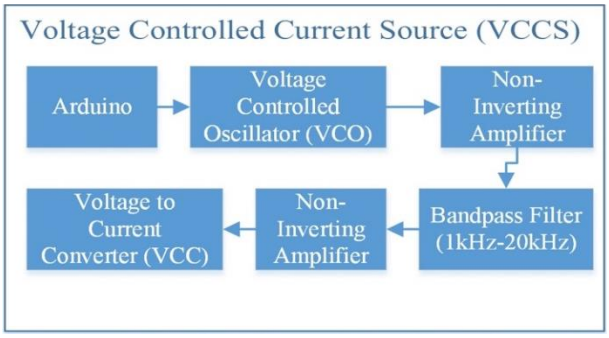


Fig. 2: Voltage Controlled Current Source (VCCS) Circuit Design.

The VCCS design has a fully digital control for controlling the frequency of the current source due to this current source is controlled by voltage, so that the frequency and magnitude of the current are easily regulated with Arduino.

2.1.2. Multiplexer and demultiplexer design

Multiplexer/Demultiplexer (Mux/Demux) in this study used IC AD506AKNZ to support 1 to 16 channels. The number of ICs used was four pieces with two pieces for current signal injection and two for voltage measurement. The switch of the Mux/Demux programmed with Raspberry pi 3 Model B and adjusted to the data measurement method. The multiplexer has two modes. The first mode is a demultiplexer, a condition for one signal input to be distributed over more than one channel. This mode is called signal injection mode to inject the constant current to practical phantom. After that, the second mode is a multiplexer. This mode is a measurement mode for determining the response of boundary voltage. Contrary to the demultiplexer, multiplexer captures signals from many channels to become an output, as shown in Figure 3.

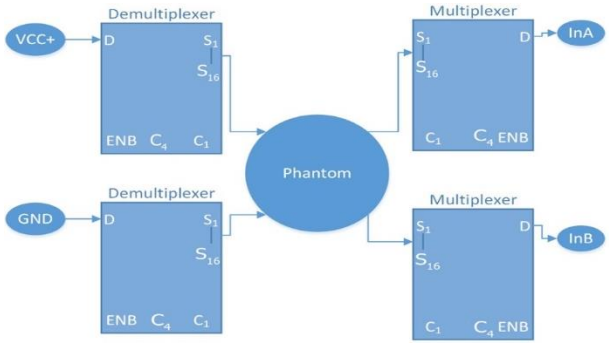


Fig. 3: Multiplexer/Demultiplexer Design for High-Speed EIT System.

This multiplexer used 16 channels with four digital controls. The pattern and speed are digitally arranged by Raspberry Pi Model B using Python programming. The pattern used is the neighboring method with a total of 256 data.

2.1.3. Voltage measurement

There are three main circuits in the voltage measurement unit, namely demodulator, peak detector, and Analog to Digital Converter (ADC) as shown in Figure 4. Demodulator circuit was used to modulate voltage from measuring the voltage by two electrodes that connected to a multiplexer circuit. This circuit compares the voltage signal between the two electrodes and can be reduced the noise measurement in the electrodes. The measurement system in the demodulator, i.e., the sample and hold are similar to the process on the DAC and ADC when sampling the signal. In this study, IC AD625KN was used because of its reliability as a demodulator in the EIT system.

Voltage data coming out of the demodulator circuit is a sinusoidal signal. The peak detector circuit is used to detect the signal peak that carried by the modulator and will be converted to the DC voltage value so that ADC can read it before entering the processing unit. In this study, we used a 16-bit Analog to Digital Converter (ADC) circuit. 16 bit ADC means the number of slice sampling voltage is 2^{16} = 65,536 discrete signals so that it can detect changes in anomalies more accurately. Moreover, responsiveness, there is a small change to input the signal with a small amplitude. In this study, IC ADS1115 was used due to it can perform conversions at data rates up to 860 samples per seconds (SPS).

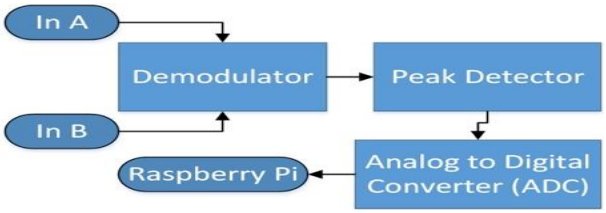


Fig. 4: Voltage Measurement Diagram.

2.2. Software development

In this study, we developed software for supporting hardware system. The software development consists of an image reconstruction algorithm, a Graphic User Interface (GUI) and a circuit controller; the explanation for each section is as follows:

a) Image reconstruction

Three main parts were used to develop the image reconstruction algorithm, namely the Finite Element Method (FEM), Jacobian Matrix, and Gauss-Newton method. FEM was used to create a mesh in the two-dimensional practical phantom model. Meanwhile, the Jacobian matrix, or also called the sensitivity matrix, was used to calculate and determine the derivatives of the measured voltages from the practical phantom respect to conductivity. Furthermore, the Gauss-Newton algorithm was used to regularise models of the EIT inverse problem for generating a reconstructed image from the conductivity distribution of 2D phantom models.

b) Graphical User Interface (GUI)

The developed GUI was intended to make the results of image reconstruction more interactive for users in the seven-inch display. The GUI split into two screens, the first one is for displaying the measured data from the boundary voltage (forward problem), and the second one presented the reconstructed image from the inverse problem process. All data could be monitored in real time condition during the data acquisition process. If there is an error in the measurement, it will be seen in the GUI.

c) Circuit Controller

In the manufactured EIT, there is a digitally controlled circuit that is VCO, Multiplexer, and ADC. The programming code has been uploaded to the control units both in Raspberry Pi and Arduino. The programming code converted by the machine to digital signals to control all electrical circuits. The control that is done is the control of frequency, pattern, port usage, and speed. With the presence of digital controls, the hardware is more flexible and can be easily managed.

2.3. Phantom design

The practical phantom design used a petri dish made from an acrylic with circular shape and had a diameter was at 90 mm, and the electrode size was 5 × 5 mm^2 that amounted to 16 electrodes (Cu electrode) and filled with the solution of NaCl 0.9% (w/v) is shown in Figure 5.

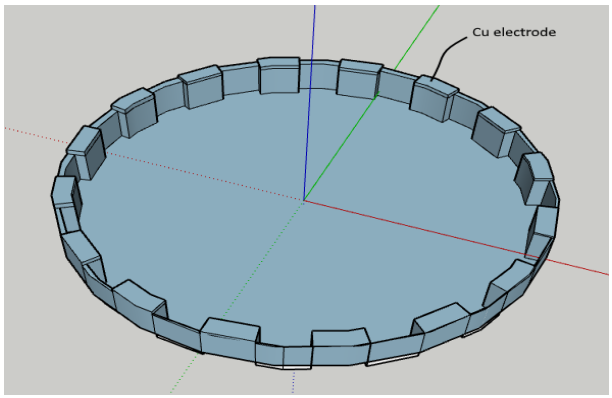


Fig. 5: The Practical Phantom for the Manufactured EIT That Equipped with 16 Electrodes.

In this study, Polyvinyl Chloride (PVC), aluminum and polyethylene (PE) were used to determine conductivity distribution on the phantom as anomalies are shown in Figure 4. The anomaly acts as an inhomogeneous condition to test the performance of the EIT system in detecting the presence of inhomogeneous objects. The selection of these three anomalies is based on the category of testing EIT capabilities that distinguishes the type of object based on electrical properties, object position, and object size. Aluminum represents as a conductive object, and the rest is a resistive object, and each anomaly will be used to test varies position inside the phantom. Position variation is based on the position of the object against the nearest electrode number. The electrode number was 1 - 16 rotate in a clockwise direction.

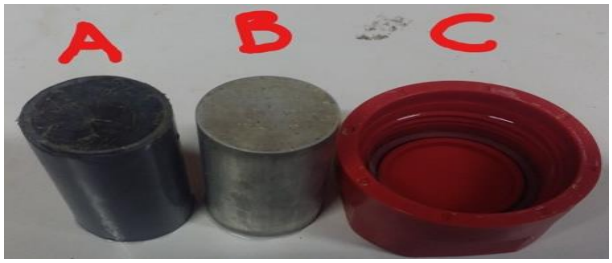


Fig. 6: Anomalies That Used to Test the Ability Of EIT (A) Polyvinyl Chloride (PVC), (B) Aluminium, and (C) Polyethylene (PE).

3. Results and discussion

3.1. Manufactured EIT system

The complete system of EIT is shown in Figure 7. Three main parts, namely hardware, software, and practical phantom, have been successfully fabricated and tested.

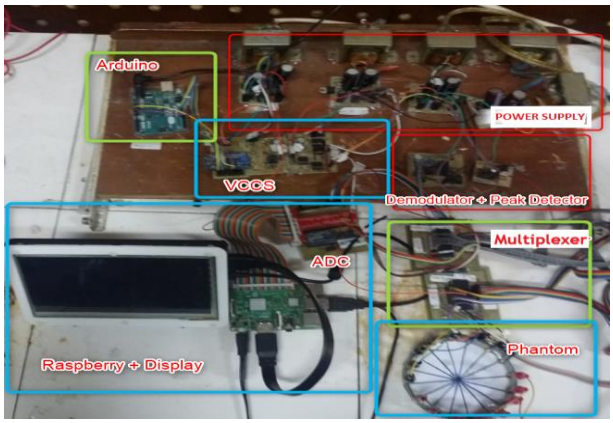


Fig. 7: VCCS Load Ranging From 1 □ 100 KΩ That Used to Conduct Test the Ability Of EIT for Supporting High Impedance Tissue.

The EIT system produces a stable current source at 1 mA 20 kHz that can support load impedance up to 2.8 kΩ, with a frequency range of 1 – 100 kHz. In this study, the EIT system was set to a single frequency at 20 kHz.

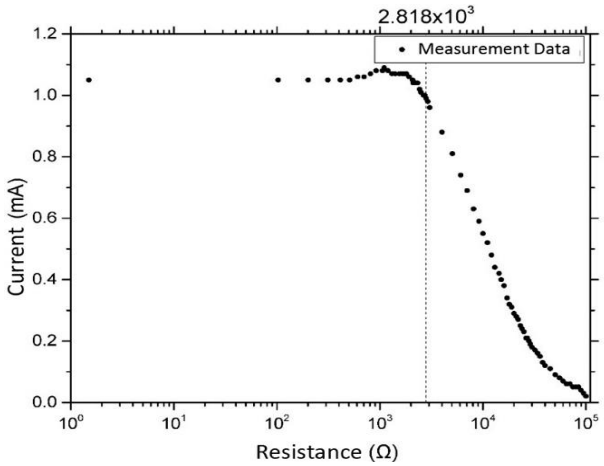


Fig. 8: VCCS Load Ranging from 1 – 100 KΩ That Used to Conduct Test the Ability of EIT for Supporting High Impedance Tissue.

Figure 8 shows the load impedance test for the manufactured EIT. It can be analyzed from the figure that the output of VCCS will be dropped below 1 mA when the VCCS has a load impedance at 2.8 kΩ. However, the current decrement is not significant. The decreased in current occurred due to the dissipation of electrical energy in the resistor and changes into heat or other forms. The higher the resistance causes, the more significant the energy dissipation that causes in weakening the amplitude of the current signal.

Moreover, the EIT system in this study supports high speed with 1 ms/data speed so that it takes 3.68 seconds for complete data acquisition using the neighboring method. The results for the speed test for data acquisition is summarised in Table 1. It seems that the system can support high-speed data acquisition without losing data. This fact showed that the system has a potential application as real-time data acquisition. This system is also equipped with processing data to images reconstruction embedded in the system. The measured data from the practical phantom could be processed into the reconstructed image took 4 seconds with a grid density of 12 circles.

In the EIT system that has been manufactured able to retrieve voltage data from the phantom (forward problem) and reconstruct the image (inverse problem) takes less than 7 seconds. The manufactured EIT less speed compared to the previous study conducted by [13], in their experiment was reported that reconstructed image speed was less than 0.3 seconds. This fact is very reasonable due to the manufactured EIT was not used personal computers (PC) but used Arduino and Raspberry Pi as a central processing unit (CPU) for data acquisition and image reconstruction.

Table 1: The Ability to Manufactured EIT When Acquiring 256 Data

No	Raspberry Speed (ms/data)	Actual time (s)
1	100	31.26
2	75	30.99
3	50	23.87
4	25	12.25
5	1	3.68

The EIT system has been equipped with a 7-inch screen with an informative GUI to monitor voltage measurement data and image reconstruction from monitored phantom conditions, as shown in Figure 9. The screen is divided into two windows to monitor voltage data and image reconstruction results from measured conductivity distributions of the phantom.

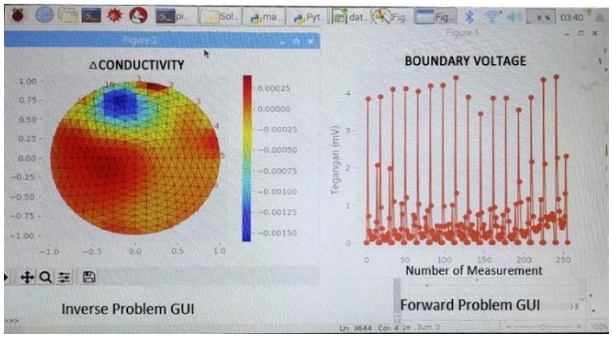


Fig. 9: Graphics User Interface (GUI) for the Manufactured EIT.

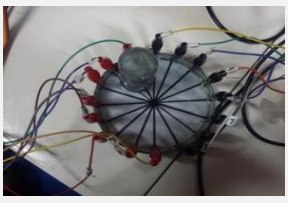
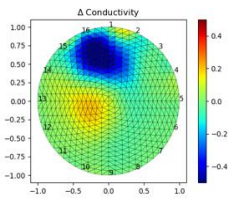
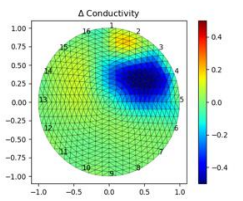
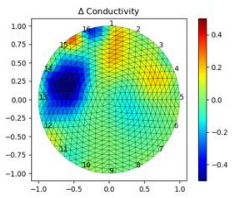
The color bar in the reconstructed image windows in Figure 9 used to show whether the anomaly object inside phantom is conductive or resistive. The red color indicates that the object anomaly is conductive, whereas the blue color shows the object has resistive properties.

3.2. The reconstructed image in the EIT system

3.2.1. Anomaly test for various positions

Table 2 shows the results of testing the position variations of PVC anomalies placed in various positions. It can be analyzed that the real position of PVC inside the phantom showed the same position in the reconstructed image on the screen monitor and had a blue color, that is mean the object is resistive. It indicated that the EIT system could be used to interpret not only the position of an object inside the phantom but also the properties of the object.

Table 2: Various Positions Test Inside the Practical Phantom Using PVC Anomaly

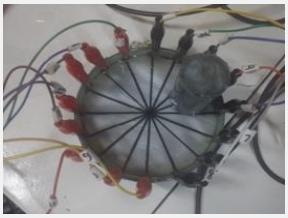
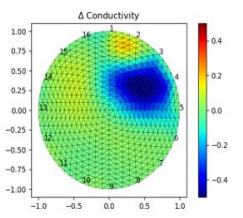
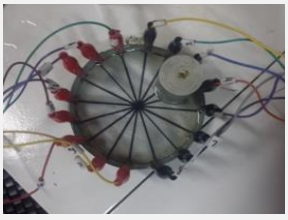
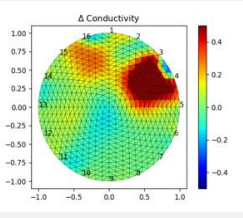
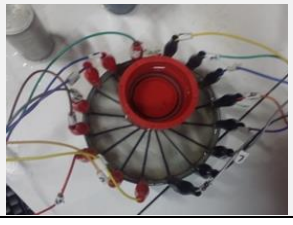
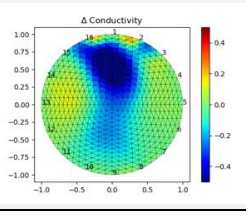
No	The practical phantom	Reconstructed image
1		
2		
3		

The principle of detecting anomalies for all points inside the phantom is based on different measurement in boundary voltage that detected at the nearest electrode with the other electrodes, and it is also compared to without anomaly condition (homogeneous) and with an anomaly condition (inhomogeneous). The uses of the principle of the voltage difference between electrodes have the same principle as magnetic resonance imaging (MRI). By measuring the voltage with the neighboring pattern, it will be known the response in each electrode point. Moreover, the exact position of the anomaly will be detected and assisted by the computation of the Gauss-Newton algorithm; the voltage difference data can be presented in the form of an image with a conductivity scale.

3.2.2. Material identification

In the study, we used three types of material to test the performance of the manufactured EIT system. The ability of manufactured EIT to identify properties of the material sample is summarized in Table 3. It can be concluded from the table that the reconstructed image showed that the manufactured EIT could be used to identify the object correctly. It can be seen that both samples of PVC and PE had a blue color, which means both objects are resistive, whereas the aluminum looks red, which shows is conductive. These results tend similarly to the previous study conducted by [8].

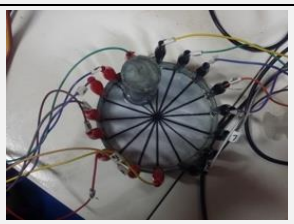
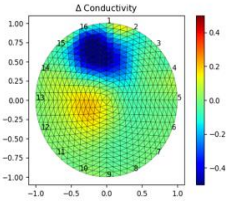
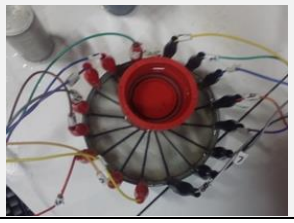
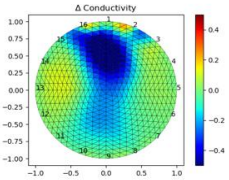
Table 3: Material Identification Test Based on Electrical Properties

No	The practical phantom	Reconstructed image
1		
2		
3		

3.2.3. Size of object anomaly

The ability of manufactured EIT in recognize the size of object anomaly inside the practical phantom is needed. Reconstructed image from manufactured EIT in determining the actual size of object anomaly is shown in Table 4. Table 4 revealed the difference in size between PVC and PE anomalies that seen from the wider blue color distribution in the reconstructed image of PE, but for regularity, their shape and size have not been achieved.

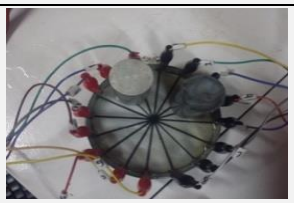
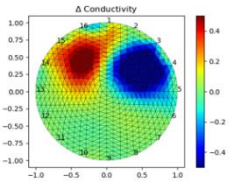
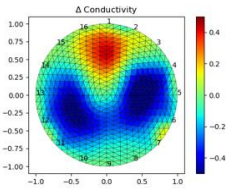
Table 4: Size Identification Test Using the Manufactured EIT

No	The practical phantom	Reconstructed image
1		
2		

3.2.4. Investigating multi-target imaging

The reconstructed image from the object with has various properties was conducted successfully in the study. Table 5 shows the summarise results from a reconstructed image from the object with different in the electrical properties, size and position.

Table 5: Multi-Target Anomalies for Multi-Target Imaging Using the Manufactured EIT

No	The practical phantom	Reconstructed image
1		
2		

It can be analyzed that the manufactured EIT can detect all anomalies inside the phantom, but it has a limitation for detecting in actual size from the object. Another limitation that occurred is the ability to distinguish the object with the same of almost the electrical properties. In this study, we used PVC and PE that had a resistivity value at $10^{14} – 10^{16}$, $10^{16} – 10^{20}$ Ω.cm, respectively. Manufactured EIT has not significantly able to distinguish the two objects in the colors formed when they are simultaneously in the phantom.

4. Conclusion

In this study, an EIT system was produced for the reconstruction of anomalous object images by varying in electrical properties, position, and size have been successfully carried out. This system can reconstruct images in one process for less than 7 seconds. Despite having limitations in identifying objects in phantoms, the system has been able to recognize objects well for their electrical position and properties. In addition, the system that has been produced has advantages in the design of cheap and portable hardware. The system that has been manufactured having the potential to be developed for the real-time system in the reconstruction of the image so that it is useful for the diagnosis of diseases in the human body.

Acknowledgment

All authors would like to thank the Indonesia Government, Ministry of Research, Technology and Higher Education and Institut Teknologi Sepuluh Nopember (ITS) Surabaya, Indonesia for providing the Postgraduate Research Grant 2018, Contract Number: 971/PKS/ITS/2018.

References

[1] A. B. S. Umbu and Endarko, "The design of voltage controlled current source (VCCS) for single frequency Electrical Impedance Tomography (EIT)," in Proceedings - 2017 International Seminar on Sensor, Instrumentation, Measurement and Metrology: Innovation for the Advancement and Competitiveness of the Nation, ISSIMM 2017, 2017, vol. 2017–Janua. https://doi.org/10.1109/ISSIMM.2017.8124256.

[2] P. O. Gaggero, "Miniaturization and Distinguishability Limits of Electrical Impedance Tomography for Biomedical Application," no. June, p. 272, 2011.

[3] C. L. Yang, "Electrical impedance tomography: algorithms and applications," thesis, Univ. Bath, 2014.

[4] A. J. Puspitasari and Endarko, "Study of precision constant current sources with resistor load and a cole-cole load for multi-frequency in electrical impedance tomography," in Proceeding - 2016 International Seminar on Sensors, Instrumentation, Measurement and Metrology, ISSIMM 2016, 2017. https://doi.org/10.1109/ISSIMM.2016.7803713.

[5] J. A. G. Gnecchi, "Voltage Controlled Current Source (VCCS) for Electrical Impedance Tomography (EIT) measurements in the α and β dispersion frequency ranges," Proc. - 2010 IEEE Electron. Robot. Automot. Mech. Conf. CERMA 2010, pp. 677–681, 2010.

[6] S. Russo, S. Nefti-Meziani, N. Carbonaro, and A. Tognetti, "Development of a High-Speed Current Injection and Voltage Measurement System for Electrical Impedance Tomography-Based Stretchable Sensors," Technologies, vol. 5, no. 3, p. 48, 2017. https://doi.org/10.3390/technologies5030048.

[7] S. Zhang, G. Xu, H. Wu, D. Geng, and W. Yan, "Multi-frequency EIT hardware system based on DSP," Annu. Int. Conf. IEEE Eng. Med. Biol. - Proc., pp. 6677–6680, 2006.

[8] M. Khalighi, B. Vosoughi Vahdat, M. Mortazavi, and A. M. Mikaeili, "Design and Implementation of Precise Hardware for Electrical Impedance Tomography (Eit)," Trans. Electr. Eng., vol. 38, no. E1, pp. 1–20, 2014.

[9] A. Adler, T. Dai, and W. R. B. Lionheart, "Temporal image reconstruction in electrical impedance tomography," Physiol. Meas., vol. 28, no. 7, p. S1, 2007. https://doi.org/10.1088/0967-3334/28/7/S01.

[10] T. Rymarczyk and K. Szulc, "Reconstruction of conductivity distribution in electrical impedance tomography by topological derivative," 2017 18th Int. Symp. Electromagn. Fields Mechatronics, Electr. Electron. Eng. ISEF 2017, vol. 1, no. x, 2017. https://doi.org/10.1109/ISEF.2017.8090755.

[11] M. Farha and Endarko, "Combined algorithm of total variation and gauss-Newton for image reconstruction in two-dimensional Electrical Impedance Tomography (EIT)," in Proceedings - 2017 International Seminar on Sensor, Instrumentation, Measurement and Metrology: Innovation for the Advancement and Competitiveness of the Nation, ISSIMM 2017, 2017, vol. 2017–Janua. https://doi.org/10.1109/ISSIMM.2017.8124257.

[12] B. Liu et al., "pyEIT: A python-based framework for Electrical Impedance Tomography," SoftwareX, vol. 7, pp. 304–308, 2018. https://doi.org/10.1016/j.softx.2018.09.005.
[13] H. Wu, Y. Yang, P. O. Bagnaninchi, and J. Jia, "Electrical impedance tomography for real-time and label-free cellular viability assays of 3D tumour spheroids," Analyst, vol. 143, no. 17, pp. 4189–4198, 2018. https://doi.org/10.1039/C8AN00729B.